

Dark-field microscopy studies of polarization-dependent plasmonic resonance of single gold nanorods: rainbow nanoparticles†

Youju Huang and Dong-Hwan Kim*

Received 30th March 2011, Accepted 12th May 2011

DOI: 10.1039/c1nr10336a

Orientation sensors require the monitoring of polarization-dependent surface plasmons of single nanoparticles. Herein, we present both the longitudinal and transverse surface plasmonic resonance from a single gold nanorod (AuNR) using conventional dark-field microscopy. The relative peak intensities of the transverse and longitudinal surface plasmons of a single AuNR can be successfully tuned by polarized excitation, which is an important step towards the use of transverse plasmon resonance of single AuNRs without photo-induced reshaping of nanoparticles. More interestingly, compared with AuNRs with small diameters, unique optical properties from AuNRs with diameters greater than 30 nm are revealed. As a result, optical images with different colors, rainbow nanoparticles (sea green, brown, red, yellow and green), depending on the polarization angle, can be revealed by a single AuNR. This result holds great promise for polarization-controlled colorimetric nanomaterials and single particle tracers in living cells and microfluidic flows.

1. Introduction

Due to their unique catalytic, photothermal and optical properties, gold nanorods (AuNRs) have been actively exploited for applications in information storage,¹ nanomedicine^{2–4} and biosensors.^{5–7} Well-defined anisotropic AuNR shapes offer two discrete localized surface plasmon resonances (LSPRs): the longitudinal and transverse modes. Only the former, however, has attracted considerable attention in the past few years^{4,8–11} due to tunable plasmon resonance over the visible to infrared regions and high sensitivity to the local refractive indices (RIs) of the surrounding medium.^{12,13} Since the introduction of potential applications of the transverse mode of anisotropic nanoparticles, a number of theoretical and experimental analyses of anisotropy of nanoparticles have been reported. In fact, conventional UV-visible instruments facilitate the detection of the transverse surface plasmon resonance of ensemble AuNRs. However, due to ensemble averaging of nanoparticles in a heterogeneous system, the obtained LSPR responses lack conformational information from the anisotropic nanoparticles. In addition, it has been a longstanding challenge to observe and acquire the transverse band of single nanoparticles by dark-field imaging, mainly due to the small cross-sections involved.^{14,15} According to the theory of light scattering, the scattering cross-section mainly depends on a nanoparticle's radius¹⁶ and the scattering of nanoparticles with diameters of 30 nm or less

cannot be distinguished from the scattering of the surroundings.¹⁷ The diameter of synthesized AuNRs by seed-mediated growth and electrochemical methods is typically in the range of 10 to 30 nm.¹⁷ Thus, a deliberate study of the transverse surface plasmon resonance of single AuNRs has remained elusive. Recently, new techniques, including dark-field microscopy,^{18,19} photothermal spectroscopy,^{6,20} near-field scanning optical microscopy²¹ and total internal reflection microscopy,^{22,23} have been demonstrated to be powerful tools to directly study the optical properties of single metallic nanoparticles. For example, Chang and co-workers successfully observed the transverse mode of AuNRs for applications in orientation sensors to study conformations and dynamics of biological systems.⁶ In Chang's study, polarization-sensitive photothermal imaging was employed to visualize AuNRs with a mean width of 25 nm and a length of 73 nm and to detect their transverse surface plasmons. In this nanoparticle size regime, absorption-based photothermal imaging is expected to be better suited to surface plasmon monitoring compared with scattering-based dark-field spectroscopy. In photothermal imaging, nanoparticles are illuminated by a laser. Therefore, it is difficult to completely avoid photo-induced reshaping of metallic nanoparticles during observation,^{1,6,24,25} which potentially leads to altered plasmonic properties of single nanoparticles. It would therefore be highly desirable to explore the transverse surface plasmon resonance of single nanoparticles using dark-field spectroscopy, which employs a broad band light source, thus this technique does not induce the deformation of objects during observation. Moreover, dark-field imaging has recently become the most widely used technique for studying the optical properties of single nanoparticles.^{13,18,19,26,27}

School of Chemical and Biomedical Engineering, Nanyang Technological University, 637457, Singapore. E-mail: dhkim@ntu.edu.sg; Fax: +65 6791 1761; Tel: +65 6790 4111

† Electronic supplementary information (ESI) available. See DOI: 10.1039/c1nr10336a

In this article, a series of AuNRs with diameters varying from 19 to 41 nm were prepared by a modified overgrowth method to explore the cut-off diameter regime where the scattering signal of the transverse mode could be observed by dark-field spectroscopy and to understand the transverse signals under polarized conditions. The anisotropy of AuNRs is conducive to the tunable relative intensities of the transverse and longitudinal peaks of a single AuNR by polarized excitation. The unique optical properties of single AuNRs with diameters greater than 30 nm discovered by dark-field imaging should open a door to the study of the fundamental phenomena of the transverse mode of single nanoparticles and the use of anisotropic characteristics of AuNRs for real world applications.

2. Results and discussion

To independently study the transverse and longitudinal surface plasmon under conventional dark-field microscopy, the overgrowth method,^{28–30} which directly controls the diameter of the AuNRs, was used. SEM images of AuNRs with different diameters are shown in Fig. 1. AuNR-19, with an average diameter of 19 nm and an average length of 48 nm, was obtained by the classic seed-mediated growth method (Fig. 1a). AuNR-29, AuNR-37 and AuNR-41 were obtained by growing AuNR-19 uniformly in all directions *via* the modified overgrowth method. After overgrowth, the average diameter of AuNR-19 increased to 29, 37 and 41 nm, depending on the amount of growth solution. The aspect ratio of the overgrown AuNRs decreased slightly because the growth rate was approximately equivalent in both the longitudinal and transverse directions.

Detailed information on the average sizes and aspect ratios of each set of AuNRs is shown in Table S1 (ESI†). The UV-Vis spectra of the AuNR ensemble (Fig. S1 in the ESI†) with different sizes show a good agreement with the data on the size of the AuNRs: an expanded diameter leads to a slight red shift of the transverse peak. Regardless of the size of the AuNRs tested in the present study, the anisotropic shape of the AuNRs produces two discrete peaks in the UV-Vis spectrum

corresponding to the longitudinal and transverse scattering of the AuNRs.

Based on the dimensional information of the synthesized AuNRs, dark-field images of single AuNRs with four different diameters along with their corresponding LSPR spectra (Fig. 2) were captured by dark-field microscopy with a color CCD camera. This allowed us to monitor the size-dependent longitudinal and transverse scattering of single AuNRs. The single AuNRs exhibit red scattering spots in the dark-field images due to predominant longitudinal scattering compared with weak transverse scattering. In good agreement with theoretical approaches and previous observations,^{9,26} AuNR-19 and AuNR-29 show clear longitudinal scattering signals but no transverse signals (Fig. 2a' and b'). In contrast, relatively weak and broad transverse bands peaking at approximately 550 nm become visible for AuNR-37 along with evident longitudinal peaks ranging from 650 to 713 nm (Fig. 2c'). AuNR-41 reveals distinct transverse peaks at approximately 560 nm (Fig. 2d'). The slight red shift of the transverse peak of the AuNRs from 550 to 560 nm could be attributed to the increase in diameter between AuNR-37 (37 nm) and AuNR-41 (41 nm), which is in good agreement with the observation from AuNR ensemble and simulated analyses.^{30,31} In principal, as the diameter of a single AuNR increases, the intensity of the transverse scattering increases. This

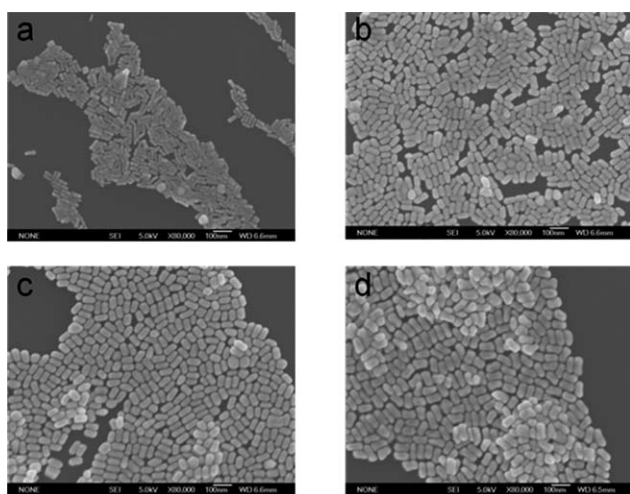


Fig. 1 Representative SEM images of AuNRs with different diameters (AuNR-19 (a), AuNR-29 (b), AuNR-37 (c) and AuNR-41(d)) obtained by the seed-mediated (a) and overgrowth (b–d) methods.

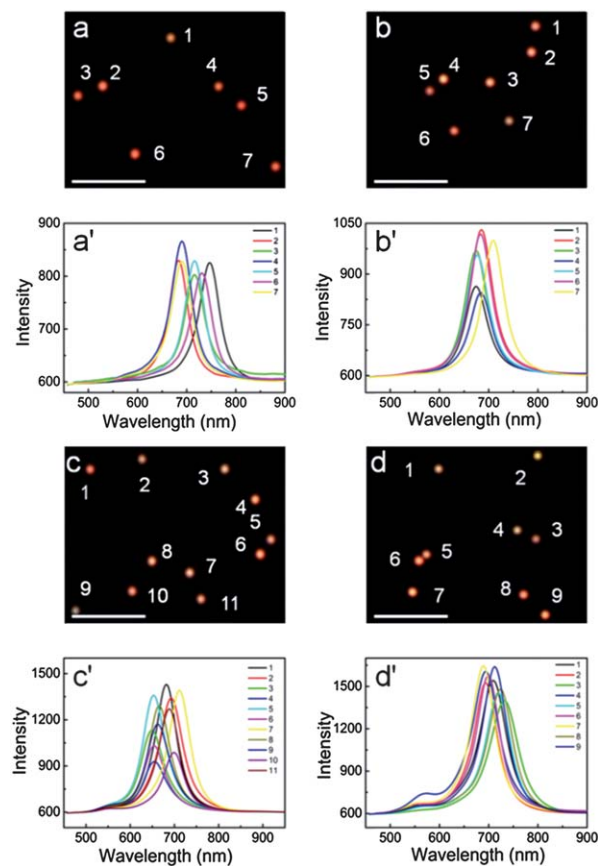


Fig. 2 Dark-field images of single AuNRs with different diameters (the AuNRs used in a, b, c and d images are from samples AuNR-19, AuNR-29, AuNR-37 and AuNR-41, respectively) and their corresponding LSPR spectra (a'–d'). The scale bars represent 5 µm.

theoretical expectation is proved experimentally by dark-field microscopic observation for the first time in the present study. In addition, the transverse plasmon resonance of single AuNRs has not previously been observed by dark-field imaging techniques.

It is expected that the longitudinal and transverse surface plasmon resonance of single AuNRs can be tuned by excitation from polarized light due to their anisotropy. Zijlstra and co-workers¹ have successfully demonstrated true five-dimensional optical recording by exploiting the polarization sensitivity of the longitudinal surface plasmon resonance of AuNRs. Ming and co-workers³² have reported strong polarization dependency of the longitudinal surface plasmon resonance of single AuNRs and enhanced fluorescence of organic fluorophores by polarized surface plasmon resonance. There has been no report, however, on the tuning of the relative intensity of the transverse surface plasmon resonance of single AuNRs due to practical difficulties in detecting the transverse surface plasmon resonance of single AuNRs. In the present study, the polarization-dependent LSPR of single AuNRs obtained by the overgrowth method was explored by polarized broad band light excitation and dynamic polarization angles from 0° to 360° in 30° intervals. Fig. 3 shows the LSPR spectra of a single AuNR (AuNR-41) without polarization and at different polarization angles.

In the absence of polarization (Fig. 3a), the transverse surface plasmon resonance peak is broad and weak. Experimental results and theoretical analyses have shown that the intensity of the longitudinal surface plasmon resonance of single AuNRs is polarization dependent and can be well fitted with a cosine squared curve.^{32–34} Our observation confirms previous reports^{32–34} by showing that the intensity changes in the longitudinal band at different polarization angles are well described by a cosine squared curve (Fig. 4).

The changes in transverse intensity of the AuNR reveal a 90° phase delay with respect to the longitudinal intensity changes. When the polarization of incident light is parallel to the long axis of the AuNR, the longitudinal intensity becomes the most dominant, and the intensity of the transverse band is barely observable (Fig. 3b). In contrast, when the polarization of incident light is orthogonal to the long axis of the AuNR, the longitudinal intensity is significantly reduced (yet still

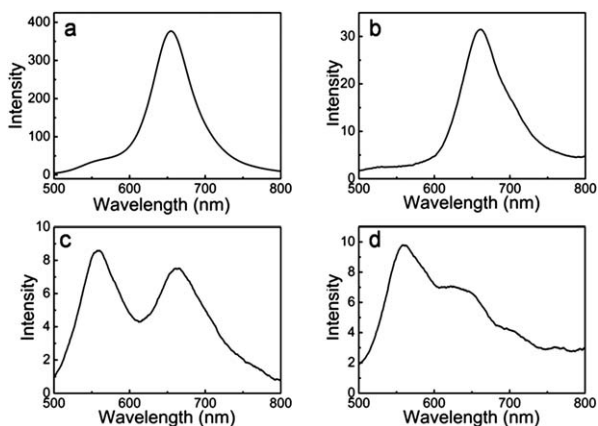


Fig. 3 Background subtracted LSPR spectra of a single AuNR (AuNR-41) without polarization (a) and with polarization at different angles (b: 60°; c: 0°; d: 150°).

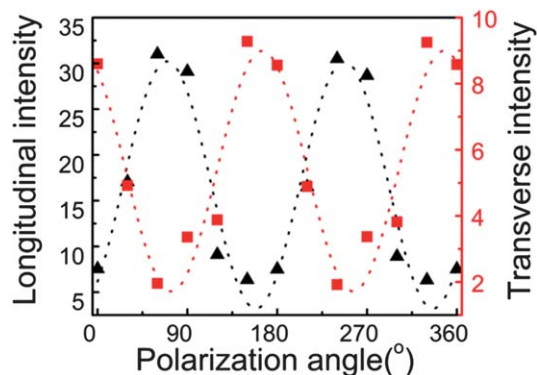


Fig. 4 The intensities in the background subtracted spectra of longitudinal (black) and transverse (red) peaks of a single AuNR-41 as used in Fig. 3 at different polarization angles ranging from 0° to 360°.

observable), and the transverse intensity becomes dominant (Fig. 3d). We note that the longitudinal intensity of the AuNR changes from 6.3 to 30.5, whereas the transverse intensity changes from 2.0 to 8.6. We independently confirmed the polarization-dependent tunability of longitudinal and transverse surface plasmonic intensities in sample AuNR-37 and AuNR-41, but this was not observable in the samples with diameters smaller than 30 nm, *i.e.*, AuNR-19 and AuNR-29. The changes in relative intensity depending on the polarization angle provide useful information for understanding the anisotropy of metallic nanoparticles. This finding makes an important step towards the use of the transverse plasmon resonance of single AuNRs because these tunable changes can be repeated over many cycles without damage and without reshaping of the measured objects.

Next, the polarization dependency of single AuNRs was further studied. Fig. 5 illustrates dark-field images of single AuNRs with different average diameters before and after polarization. The AuNRs with average diameters less than 30 nm (sample AuNR-19 and AuNR-29) show scattering spots that are red under both unpolarized and polarized conditions. Therefore, no measurable polarization-dependent characteristics are shown (Fig. 5a–a' and 5b–b'). Interestingly, although the scattering spots of single AuNRs of AuNR-37 and AuNR-41 are red without polarization (Fig. 5c and d), their corresponding scattering spots under polarized conditions exhibit different colors

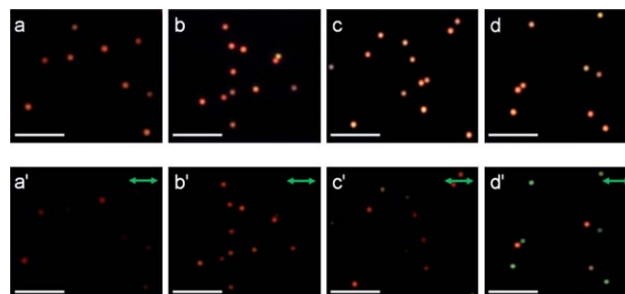


Fig. 5 Dark-field images without (a, b, c and d) and with polarization (a', b', c' and d') of single AuNRs with different diameters (the AuNRs used in a, b, c and d images are from samples AuNR-19, AuNR-29, AuNR-37 and AuNR-41, respectively). The scale bars represent 5 μm . Green double-arrows represent the incident light polarization.

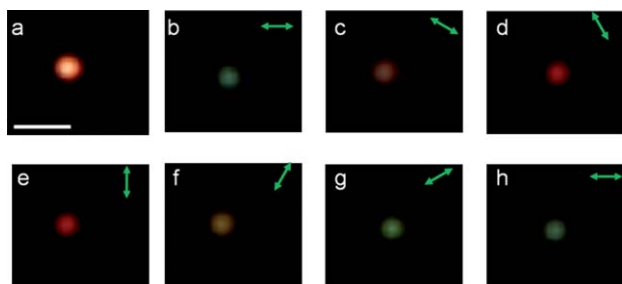


Fig. 6 Dark-field images of the single AuNR without polarization (a) and at different polarization angles (b: 0°; c: 30°; d: 60°; e: 90°; f: 120°; g: 150°; h: 180°). The scale bar represents 1 μm . Green double-arrows represent the incident light polarization.

(Fig. 5c' and 5d'). To understand this observation, we further explored dark-field images of a single AuNR at different polarization angles. A series of optical images of a single AuNR (AuNR-41) with varying polarization angles is demonstrated in Fig. 6.

It is clear that the single AuNR exhibits a variety of colors (sea green (Fig. 6b), brown (Fig. 6c), red (Fig. 6d), yellow (Fig. 6f) and green (Fig. 6g)) at different polarization angles. Obviously, these tunable colors of single AuNRs are not observable for AuNR-19 or AuNR-29 (Fig. S2 in the ESI†). In this size regime, the transverse contribution is still minute, leading the scattering spots to maintain their red color at varying polarization angles. The colors of single metallic nanoparticles in dark-field microscopy can be ascribed to their corresponding scattering spectra. For example, silver nanoparticles with triangular, pentagonal and spherical shapes exhibit red, green and blue optical images,³⁵ respectively, due to their corresponding scattering peaks at 670 nm, 530 nm and 450 nm, which independently belong to the red, green and blue regions of the visible light spectrum. Single Au-nanospheres generally have a peak at 520 nm, exhibiting green optical images,³⁶ whereas single AuNRs exhibit red scattering spots due to their predominant longitudinal surface plasmon resonance.^{9,26} The longitudinal surface plasmon resonance dominates when the polarized excitation is parallel to the long axis of the AuNR, exhibiting a red spot. The transverse surface plasmon resonance, however, becomes observable when the polarized excitation is orthogonal to the long axis of the AuNR, showing a green scattering spot, similar to the scattering of gold spheres. At other polarization angles, the colors of the dark-field images are ascribed to the collaborative contributions of both the longitudinal and transverse modes of the AuNR, leading to mixed colors with different ratios of red and green. Such tunable colors from a single AuNR are promising for polarization-controlled colorimetric nanomaterials and single particle tracers in living cells and microfluidic flows.

3. Conclusions

We have experimentally shown that single AuNRs with diameters greater than 30 nm reveal unique optical properties compared with AuNRs with smaller diameters under conventional dark-field microscopy. In particular, the relative intensity of the transverse surface plasmon resonance of single AuNRs can be tuned by polarized excitation. Due to the nontrivial

contribution from the transverse plasmon resonance, optical images with different colors (sea green, brown, red, yellow and green) can be obtained by a single AuNR. This result opens a door to the study of the fundamental phenomena of the transverse mode of single nanoparticles and the use of anisotropic characteristics of AuNRs.

4. Experimental section

4.1. Chemicals

Cetyltrimethylammonium bromide (CTAB), hydrogen tetrachloroaurate(III) trihydrate ($\text{HAuCl}_4 \cdot 3\text{H}_2\text{O}$), ascorbic acid (AA), sodium borohydride (NaBH_4) and silver nitrate (AgNO_3) were purchased from Sigma-Aldrich. All reagents were used as received.

4.2. Preparation of AuNRs

A seed-mediated growth procedure was used to obtain AuNRs with an average diameter of 19 nm and length of 49 nm (named AuNR-19).^{14,15} Briefly, 10 mL of 0.2 M CTAB solution was mixed with 10 mL of 5×10^{-4} M HAuCl_4 . Then 1.2 mL of ice-cold 0.01 M NaBH_4 was added to the mixed solution with vigorous stirring for 2 min. The obtained solution turned a brownish yellow color and was kept at room temperature for at least 10 min before use. Next, 47.5 mL of 0.1 M CTAB, 2.5 mL of 0.01 M HAuCl_4 , 300 μL of 0.01 M silver nitrate and 275 μL of 0.1 M ascorbic acid were mixed together under continuous stirring. Finally, 60 μL of the seed solution was added to the above mixture for AuNR growth. The solution was kept at room temperature for at least 10 h and centrifuged twice at 7000 rpm for 30 min. The precipitate in the plastic centrifugation tube was re-dispersed into 15 mL of distilled water.

The AuNR overgrowth method from a previous report³⁰ was slightly modified to obtain AuNRs with varying diameters, as listed in Table S1 of the ESI†. The obtained AuNRs are designated as AuNR-29, AuNR-37 and AuNR-41 and have average diameters of 29, 37 and 41 nm and lengths of 59, 63 and 75 nm, respectively. A volume of 100 mL of growth solution consisting of 0.01 M CTAB and 2.5×10^{-4} M HAuCl_4 was mixed with 555 μL of 0.1 M ascorbic acid. A pre-determined amount of growth solution (5, 7.5 and 10 mL) was transferred to three different plastic tubes. After gentle stirring for 2 min, 200 μL of AuNR-19 solution was added to each tube. The solutions were kept at 30 °C in a water bath for at least 12 h and centrifuged twice at 7000 rpm for 5 min before use.

4.3. Dark-field imaging of single AuNRs

The AuNRs were immobilized onto glass slips according to our previous work.²⁶ Briefly, the glass substrates were cleaned using 'piranha' solution (30% H_2O_2 mixed in a ratio of 1 : 3 with concentrated H_2SO_4) at 60 °C for 2 h and then washed with an excess of water and ethanol. The clean glass substrate was immersed in a diluted AuNR solution for 3 min, washed with an excess of water and ethanol, and blown dry with nitrogen. Dark-field imaging and spectroscopy on single AuNRs were carried out with an Olympus IX71 inverted microscope coupled with a color digital camera (DS-Fi1-U2 with the NIS Element

D software) and a line-imaging spectrometer (Acton Research SpectraPro2150i). The system employs an oil (refractive index of 1.516) immersion ultra-dark-field condenser (numerical aperture of 1.2–1.4) and a 100× oil immersion Plan-neofluar (Olympus) objective with an adjustable numerical aperture from 0.6 to 1.3. Illumination was provided by an integrated 100 W halogen source. A rotatable polarizer (Olympus, U-POT) was installed onto the condenser of the Olympus IX71 microscope, and the analyzer (Olympus, IX2-AN) was fixed in the slot below the mirror unit turret. The polarization angle was defined by the angle between the transmission directions of the polarizer and analyzer. The background spectra were measured in an adjacent position to the individual particles.

Acknowledgements

We gratefully acknowledge the Nanyang Technological University for support of this work. We also acknowledge financial support from the Science and Engineering Research Council (102 152 0014) and the Academic Research Funding Tier 1 (RG65/08) of Singapore.

Notes and references

- 1 P. Zijlstra, J. W. M. Chon and M. Gu, *Nature*, 2009, **459**, 410–413.
- 2 E. Boisselier and D. Astruc, *Chem. Soc. Rev.*, 2009, **38**, 1759–1782.
- 3 X. H. Huang, S. Neretina and M. A. El-Sayed, *Adv. Mater.*, 2009, **21**, 4880–4910.
- 4 M. Liu, P. H. Yang and J. Y. Cai, *Prog. Biochem. Biophys.*, 2009, **36**, 1402–1407.
- 5 J. N. Anker, W. P. Hall, O. Lyandres, N. C. Shah, J. Zhao and R. P. Van Duyne, *Nat. Mater.*, 2008, **7**, 442–453.
- 6 W. S. Chang, J. W. Ha, L. S. Slaughter and S. Link, *Proc. Natl. Acad. Sci. U. S. A.*, 2010, **107**, 2781–2786.
- 7 C. Yu, H. Nakshatri and J. Irudayaraj, *Nano Lett.*, 2007, **7**, 2300–2306.
- 8 K. M. Mayer, S. Lee, H. Liao, B. C. Rostro, A. Fuentes, P. T. Scully, C. L. Nehl and J. H. Hafner, *ACS Nano*, 2008, **2**, 687–692.
- 9 G. J. Nusz, S. M. Marinakos, A. C. Curry, A. Dahlin, F. Hook, A. Wax and A. Chilkoti, *Anal. Chem.*, 2008, **80**, 984–989.
- 10 A. Wijaya, S. B. Schaffer, I. G. Pallares and K. Hamad-Schifferli, *ACS Nano*, 2009, **3**, 80–86.
- 11 C. Yu and J. Irudayaraj, *Anal. Chem.*, 2007, **79**, 572–579.
- 12 H. J. Chen, X. S. Kou, Z. Yang, W. H. Ni and J. F. Wang, *Langmuir*, 2008, **24**, 5233–5237.
- 13 L. Guo, A. R. Ferhan, K. Lee and D. H. Kim, *Anal. Chem.*, 2011, **83**, 2605–2612.
- 14 A. Gole and C. J. Murphy, *Chem. Mater.*, 2004, **16**, 3633–3640.
- 15 B. Nikoobakht and M. A. El-Sayed, *Chem. Mater.*, 2003, **15**, 1957–1962.
- 16 *Light Scattering by Small Particles*, ed. H. C. van de Hulst, Dover Publications, 1981.
- 17 M. A. Van Dijk, A. L. Tchegotareva, M. Orrit, M. Lippitz, S. Berciaud, D. Lasne, L. Cognet and B. Lounis, *Phys. Chem. Chem. Phys.*, 2006, **8**, 3486–3495.
- 18 M. Hu, C. Novo, A. Funston, H. N. Wang, H. Staleva, S. L. Zou, P. Mulvaney, Y. N. Xia and G. V. Hartland, *J. Mater. Chem.*, 2008, **18**, 1949–1960.
- 19 Y. J. Song, P. D. Nallathamby, T. Huang, H. E. Elsayed-Ali and X. H. N. Xu, *J. Phys. Chem. C*, 2009, **114**, 74–81.
- 20 M. A. Taubenblatt, *Appl. Phys. Lett.*, 1988, **52**, 951–953.
- 21 K. Imura, T. Nagahara and H. Okamoto, *J. Phys. Chem. B*, 2004, **108**, 16344–16347.
- 22 C. Sönnichsen, T. Franzl, T. Wilk, G. Von Plessen, J. Feldmann, O. Wilson and P. Mulvaney, *Phys. Rev. Lett.*, 2002, **88**, 774021–774024.
- 23 C. Sönnichsen, S. Geier, N. E. Hecker, G. Von Plessen, J. Feldmann, H. Ditlbacher, B. Lamprecht, J. R. Krenn, F. R. Aussenegg, V. Z. H. Chan, J. P. Spatz and M. Möller, *Appl. Phys. Lett.*, 2000, **77**, 2949–2951.
- 24 S. S. Chang, C. W. Shih, C. D. Chen, W. C. Lai and C. R. C. Wang, *Langmuir*, 1999, **15**, 701–709.
- 25 R. Jin, Y. Cao, C. A. Mirkin, K. L. Kelly, G. C. Schatz and J. G. Zheng, *Science*, 2001, **294**, 1901–1903.
- 26 L. Guo, X. Zhou and D. H. Kim, *Biosens. Bioelectron.*, 2011, **26**, 2246–2251.
- 27 C. Novo, A. M. Funston, I. Pastoriza-Santos, L. M. Liz-Marzan and P. Mulvaney, *Angew. Chem., Int. Ed.*, 2007, **46**, 3517–3520.
- 28 X. Kou, S. Zhang, Z. Yang, C. K. Tsung, G. D. Stucky, L. Sun, J. Wang and C. Yan, *J. Am. Chem. Soc.*, 2007, **129**, 6402–6404.
- 29 W. Ni, X. Kou, Z. Yang and J. Wang, *ACS Nano*, 2008, **2**, 677–686.
- 30 K. Sohn, F. Kim, K. C. Pradel, J. Wu, Y. Peng, F. Zhou and J. Huang, *ACS Nano*, 2009, **3**, 2191–2198.
- 31 X. Xu and M. B. Cortie, *Adv. Funct. Mater.*, 2006, **16**, 2170–2176.
- 32 T. Ming, L. Zhao, Z. Yang, H. J. Chen, L. D. Sun, J. F. Wang and C. H. Yan, *Nano Lett.*, 2009, **9**, 3896–3903.
- 33 L. Novotny, *Phys. Rev. Lett.*, 2007, 98.
- 34 T. Itoh, K. Hashimoto and Y. Ozaki, *Appl. Phys. Lett.*, 2003, **83**, 2274–2276.
- 35 J. J. Mock, M. Barbic, D. R. Smith, D. A. Schultz and S. Schultz, *J. Chem. Phys.*, 2002, **116**, 6755–6759.
- 36 C. J. Orendorff, T. K. Sau and C. J. Murphy, *Small*, 2006, **2**, 636–639.